Chapter 6

Study of the role of some of model ingredients in asymmetric reactions induced by neutron-rich nuclei

6.1 Introduction

As reported in previous chapters, the disassembly of colliding nuclei into fragments is a complex phenomenon that depends essentially on the reaction inputs such as incident energy, colliding geometry (i.e., impact parameter), system mass, isospin as well as mass asymmetry etc. of a reaction [21, 92, 95, 125, 137, 138, 178, 231, 236, 291, 365, 366]. At lower incident energies, the available excitation energy is too small to allow the breaking of nuclei into fragments. But as the incident energy increases, colliding nuclei can disintegrate into dozens of fragments consisting of light charged particles and intermediate and heavy mass fragments [4, 20, 21, 24, 92, 95, 125, 137, 138, 178, 231, 236, 291, 365, 366]. The evolution of these different fragments (and their sizes) depends on the above mentioned reaction parameters. Extensive studies have been reported in the literature where the effects of different entrance channels and model ingredients can be found on the fragmentation pattern [4, 20, 21, 24, 137, 201, 231, 232, 235, 291, 295, 356, 366–368].

In addition to the above reaction parameters, fragmentation has also been influenced by various physical parameters such as nuclear equation of state (as discussed in the Chapter 4) [21, 137, 201, 232, 291, 295, 366] and/or nucleon-nucleon (NN) scattering cross-section [201, 231, 235, 356, 367]. For example, in Ref. [366], fragmentation of $^{197}_{79}$Au + $^{197}_{79}$Au reaction was examined within Quantum Molecular Dynamics (QMD) approach using soft and hard equations of state and marginal effect of different equations of state

was reported on multifragmentation. In another study [201], significant effect of EOS as well as its momentum dependence was observed in peripheral collisions of various nearly symmetric reactions. We have also discussed (see Chapter 4) the results of our calculations with momentum-dependent interactions for the nearly symmetric and asymmetric reactions both at central and peripheral colliding geometry and found that though the effect of MDIs vanishes at higher incident energies for central collisions, a significant effect, however, remains at peripheral colliding geometry even at higher beam energies. At the same time, some studies reported significant role of NN scattering cross section on multifragmentation. For example, Peilert *et al.* [231] studied the sensitivity of fragments's yield in the symmetric reactions of $^{93}_{41}$Nb + $^{93}_{41}$Nb and $^{197}_{79}$Au + $^{197}_{79}$Au towards in-medium NN scattering cross-section and observed marginal sensitivity of the same. Also, Puri and co-worker [356] reported an enhanced role of NN cross-section on fragment's yield at peripheral collisions contrary, to central ones where insignificant effect was observed. At the same time, various technical parameters such as interaction range (Gaussian width) also influences the dynamics of the reaction at intermediate energies. For example, Hartnack *et al.* [189] studied the role of Gaussian width and initialization on the transverse flow and fragment's yield in the reaction of $^{197}_{79}$Au + $^{197}_{79}$Au. Their findings revealed a significant role of interaction range and initialization on the fragment's mass distribution. Similar sensitivity of fragmentation towards interaction range was also reported in Refs. [369, 370] where various symmetric reactions ranging from $^{40}_{20}$Ca + $^{40}_{20}$Ca to $^{197}_{79}$Au + $^{197}_{79}$Au were simulated using molecular dynamics approach. It is worth mentioning that significant effect of these physical and technical parameters on various other phenomena such as collective flow [29], nuclear stopping [57], entropy production [291, 371] etc. has also been reported.

All the above mentioned studies are carried out for the symmetric reactions and little attention has been paid to study the dynamics of asymmetric reactions. Further, it should be noted that Puri and co-worker [232] have made a study to investigate the role of momentum-dependent interactions, NN cross-section and other model ingredients on the fragmentation in asymmetric reactions of $^{16}_{8}$O + $^{80}_{35}$Br and $^{16}_{8}$O + $^{108}_{47}$Ag. However, this study was carried out using isospin independent version of molecular dynamics approach i.e., Quantum Molecular Dynamics (QMD) model [35].

At the same time, with the advancements in the radioactive ion beam facilities (as discussed earlier), the nuclear physics community has shifted its intention to study nuclei

far away from the β-stability line. This is because of the reason that these nuclei exhibit unique features when compared with nuclei those are close to the β-stability line. Further, it is also important to understand that how the shell structure might change due to the change in the limits of stability as nuclei become more exotic. In this direction, heavy-ion collisions induced by the neutron-rich nuclei have gained a lot of interest [22]. However, the production of neutron-rich nuclei faces several difficulties such as very short half lives, low production cross-section and the production of background species along with the nuclei of interest. But modern radioactive ion beam facilities have made it possible to produce high quality radioactive ion beams. At the same time, one needs reliable theoretical tools to extract information of the EOS of neutron-rich matter from heavy-ion reactions induced by neutron-rich beams. Several transport models such as IBUU [186], SMF [188] and IQMD [189] etc. (as these models also take care of the isospin degree of freedom) have been successfully developed in recent years to study the nuclear reactions induced by the neutron-rich nuclei at intermediate energies. Also, as discussed earlier, the dynamics of symmetric and asymmetric reactions are quite different and hence, it would be interesting to see how the different model ingredients (in particular, physical parameters) affect the dynamics of asymmetric reactions having neutron-rich targets. Here, we will only probe the effects of some of the model ingredients that depend on the isospin degree of freedom (i.e., symmetry energy and NN cross section). Therefore, the aim of the present study is to shed some light on the role of isospin degree of freedom via symmetry energy and NN cross-section on the yield of fragments in the asymmetric reactions induced by neutron-rich nuclei.

6.2 Results and discussions

To investigate the effect of isospin degree of freedom via symmetry energy and NN cross section in the asymmetric reactions with neutron-rich targets, first of all, we simulated the reactions of $^{16}_{8}$O + $^{84}_{35}$Br, $^{16}_{8}$O + $^{92}_{35}$Br, $^{16}_{8}$O + $^{113}_{47}$Ag and $^{16}_{8}$O + $^{122}_{47}$Ag at 50, 75, 150, 200 MeV/nucleon. Note that we kept our projectile same and took neutron-rich targets for these reactions. Therefore, in the present study, we will mainly focus on the asymmetric reactions involving neutron-rich targets. This will also help us to understand the change in the dynamics of the reaction with respect to target neutron-richness (i.e., n/p ratio of targets) if any. We have used soft equation of state along with energy- and isospin-

dependent NN cross-section (reduced by 20%) until stated explicitly. All reactions are followed till 300 fm/c. We will first see the effect of isospin degree of freedom via symmetry energy and NN cross-section on the yield of fragments and after that we will investigate the change in the yield of fragments with n/p ratio of the target.

6.2.1 Role of isospin degree of freedom via symmetry energy and NN cross-section on the yield of fragments

In Fig. 6.1, we display the size of heaviest fragment $<A_f^{max}>$, multiplicity of free nucleons (FNs), light charged particles (LCPs) and intermediate mass fragments (IMFs) at various incident energies for the reaction of $^{16}_{8}$O + $^{84}_{35}$Br. From the figure, we see that the size of heaviest fragment $<A_f^{max}>$ decreases with increase in incident energy (see open circles) that enhances the multiplicity of FNs, LCPs and IMFs. This happens because of the violent nature of the collisions when we go towards higher incident energies. Similar results are also reported for the mass asymmetric reactions induced by the stable nuclei [24]. To see the role of isospin degree of freedom via symmetry energy, we performed calculations without symmetry energy in addition to the one with symmetry energy (Default) and results are displayed by closed squares (and labeled by E_{Sym}^{off}) in Fig. 6.1. We notice that the size of heaviest fragment now increases. This is because of the repulsive nature of symmetry energy and therefore, with less repulsion (due to the absence of symmetry energy), $<A_f^{max}>$ gets bigger. On the other hand, the multiplicities of FNs, LCPs and IMFs get decreased. We also notice that the role of symmetry energy is much more dominant at lower incident energies and it decreases as we move towards higher incident energy range. This is because of the importance of mean field at lower beam energies. Next, to see the role of isospin dependence of NN cross-section, we also performed calculations by keeping the cross-section isospin independent, i.e., the cross section for neutron-proton collisions is same as that for neutron-neutron (proton-proton) collisions. The results are displayed by crossed squares (and labeled by σ_{noniso}). From the figure, we find that keeping cross-section isospin independent results marginal effect on the yield of fragments at very higher incident energies (i.e., 200 Mev/nucleon) whereas, at low incident energies (i.e., 50 Mev/nucleon) isospin independent cross-section doesn't yield different results when compared with default calculations in the dynamics of asymmetric reactions having neutron-rich targets. These results are in accordance with the ones reported in the previous chapter.

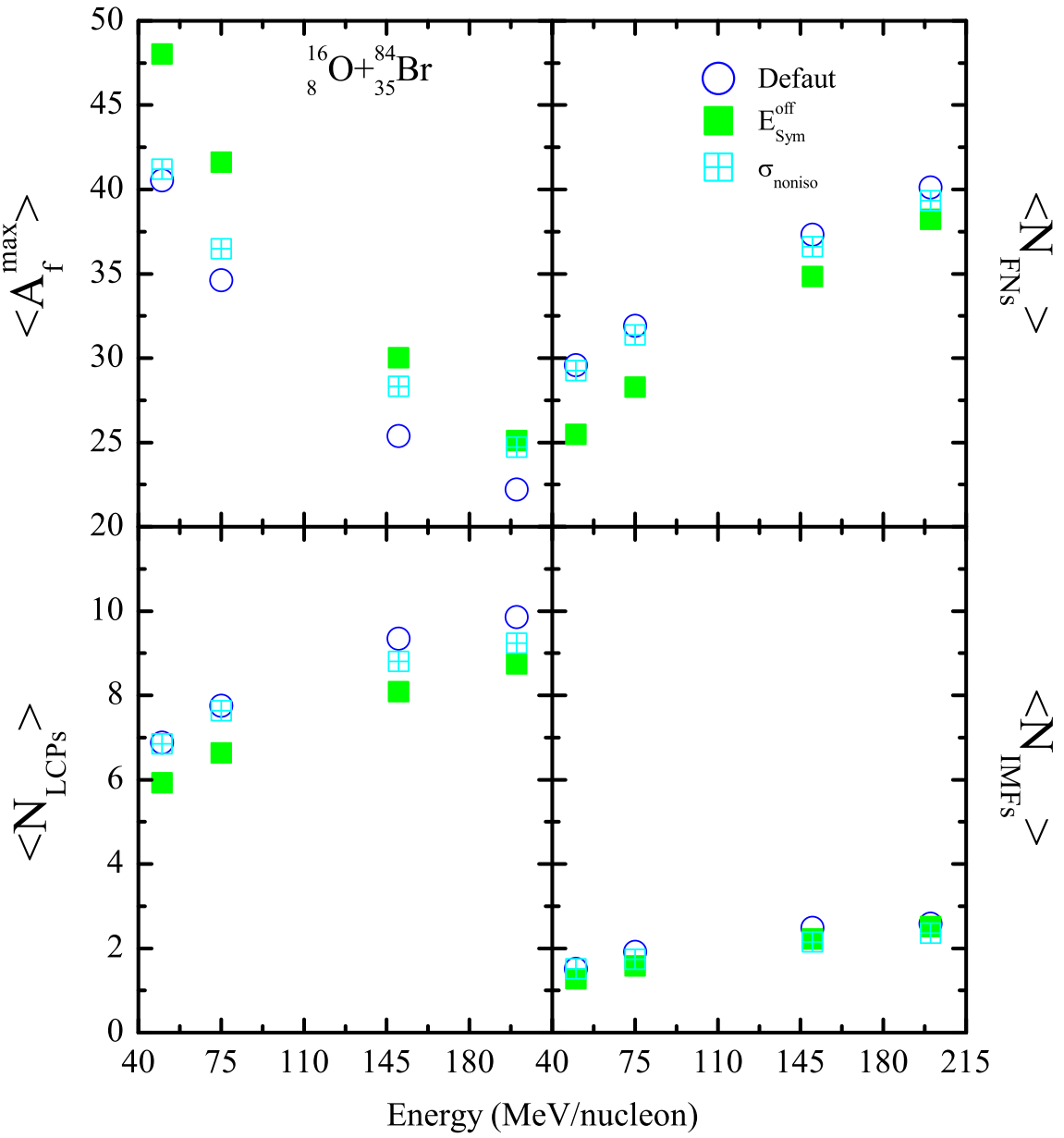

Figure 6.1: The heaviest fragment ($<A_f^{max}>$), multiplicity of free nucleons (FNs), light charged particles (LCPs) and intermediate mass fragments (IMFs) as a function of incident energy for the reaction of $^{16}_{8}$O + $^{84}_{35}$Br. Various symbols are explained in the text.

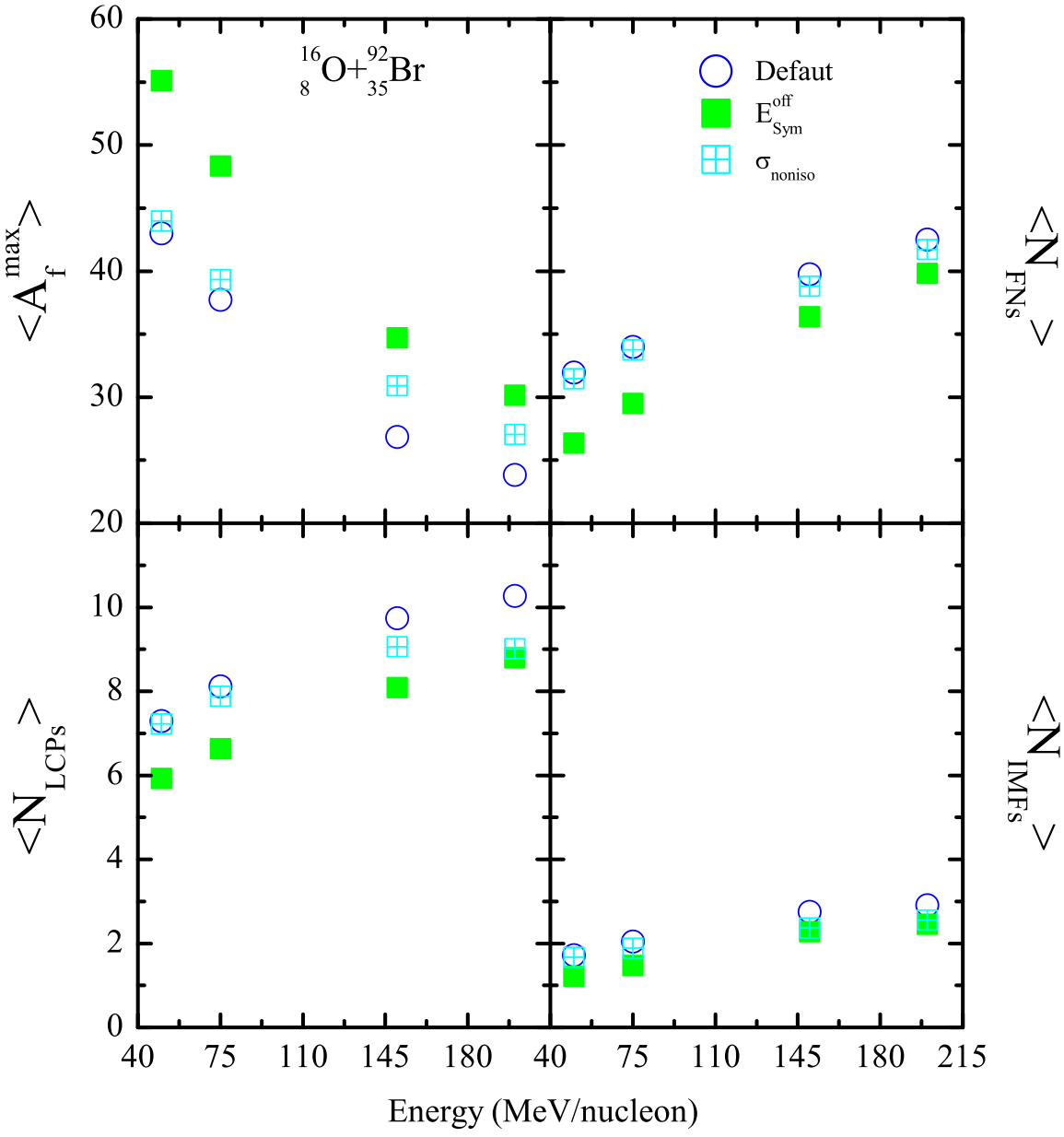

Figure 6.2: Same as Fig. 6.1, but for the reaction of $^{16}_{8}$O + $^{92}_{35}$Br.

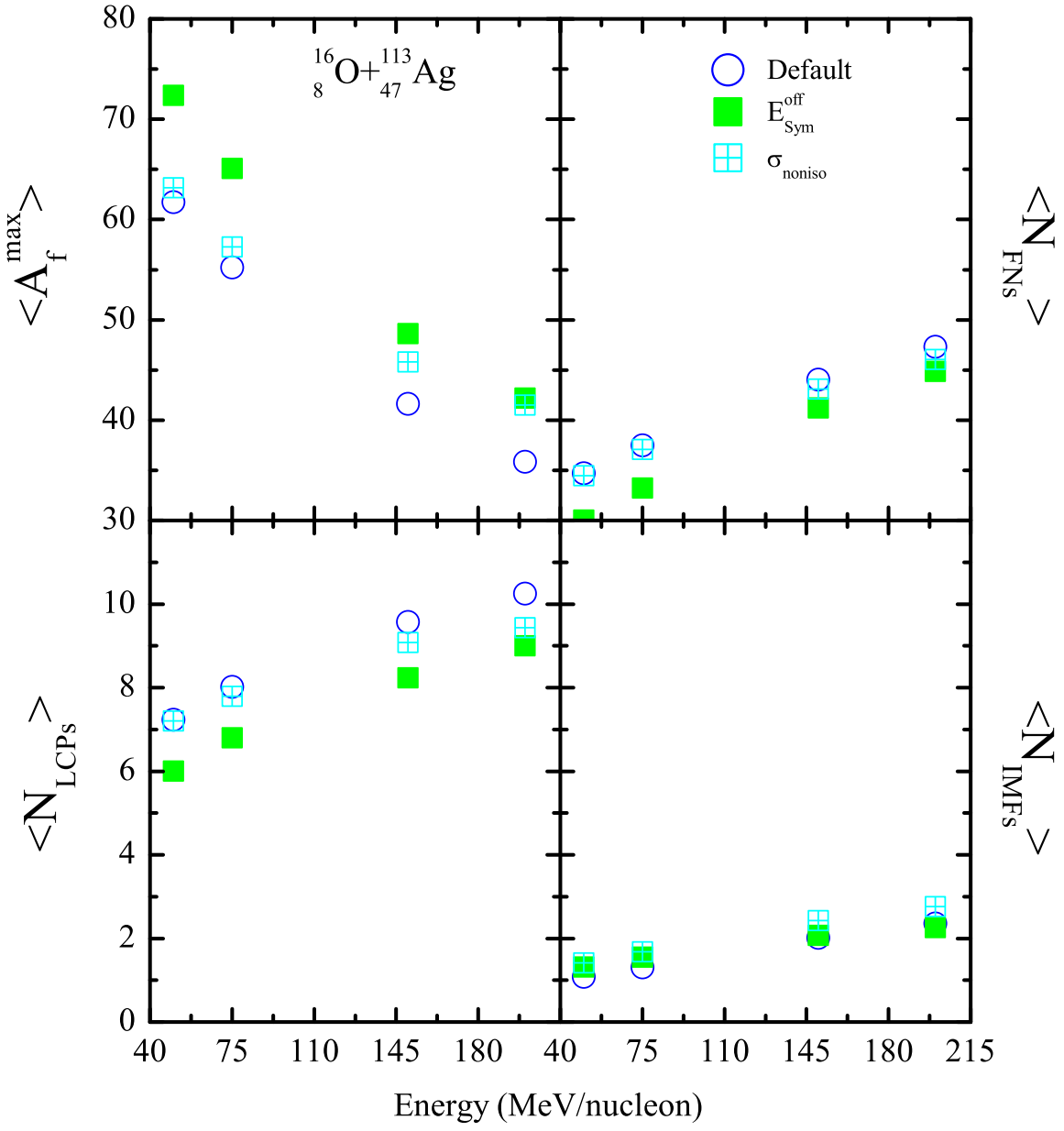

Figure 6.3: Same as Fig. 6.1, but for the reaction of $^{16}_{8}O + ^{113}_{47}Ag$.

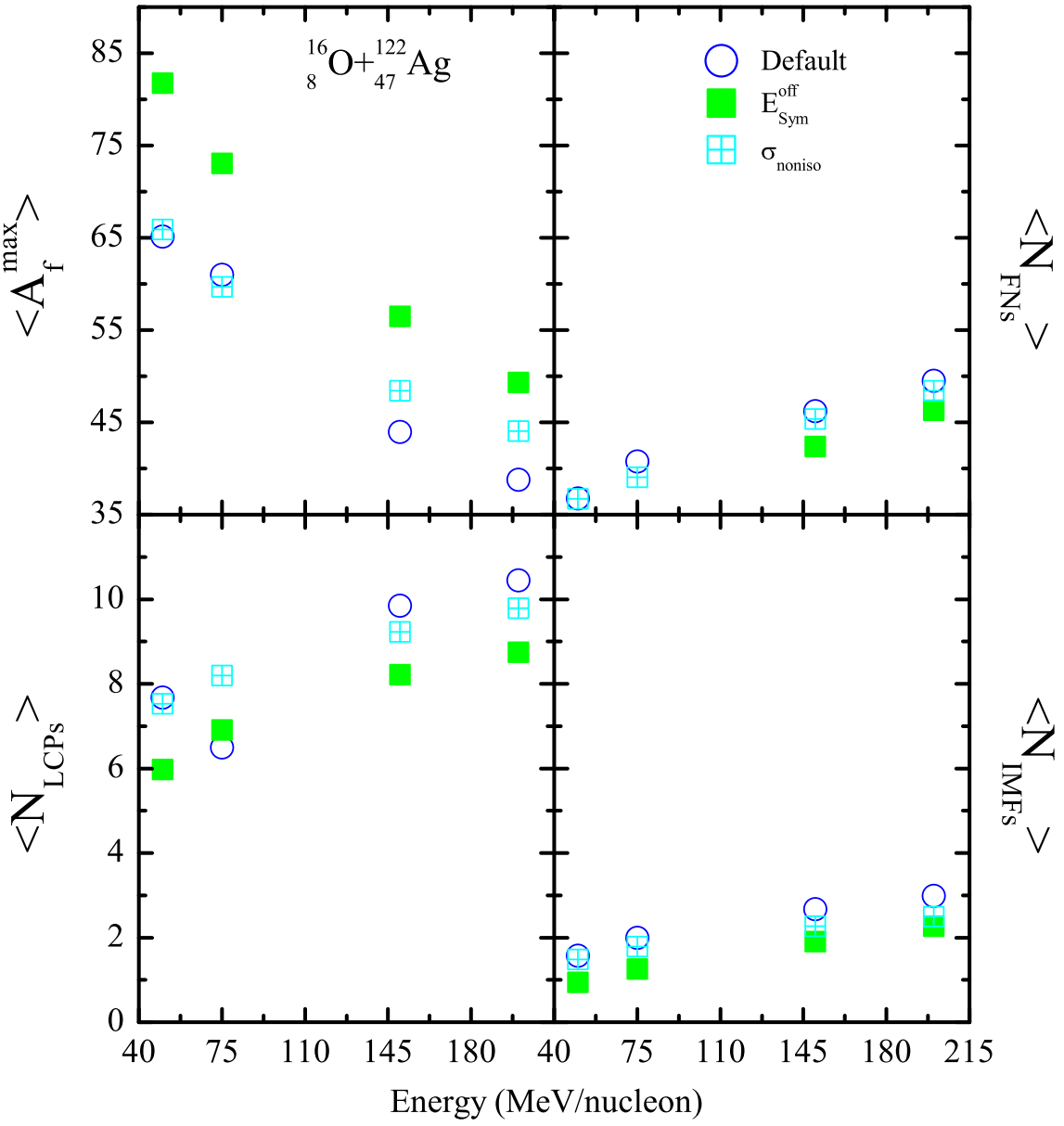

Figure 6.4: Same as Fig. 6.1, but for the reaction of $^{16}_{8}$O + $^{122}_{47}$Ag.

Next, we study the effect of isospin degree of freedom via symmetry energy and NN cross-section on the yield of fragments in the reactions of $^{16}_{8}$O + $^{92}_{35}$Br (having more neutron-rich target with respect to the target in the reaction of $^{16}_{8}$O + $^{84}_{35}$Br) and the results are shown in Fig. 6.2. Here, again three different set of parameters are used (see above). The trends observed in Fig. 6.2 are almost similar to the ones observed in Fig. 6.1. The only striking point is that with the increase in the neutron-richness (i.e., n/p ratio) of the target, isospin degree of freedom via symmetry energy shows more pronounced effect at lower incident energies.

Moving in the same direction, we also simulated the reactions of $^{16}_{8}$O + $^{113}_{47}$Ag and $^{16}_{8}$O + $^{122}_{47}$Ag and results are displayed in Figs. 6.3 and 6.4, respectively. Again, the calculations are carried out by taking three different set of parameters (i.e., default, with out symmetry energy and isospin independent NN cross-section). The trends of the observed results are again consistent with the ones reported in Figs. 6.1 and 6.2 and with the increase in the neutron-richness of the target (i.e., moving from $^{113}_{47}$Ag to $^{122}_{47}$Ag), the isospin degree of freedom via symmetry energy shows more pronounced effects at lower incident energies (as observed in Fig. 6.2). This creates curiosity to investigate the effect of n/p ratio of the target on the yield of fragments in the asymmetric reactions induced by neutron-rich targets.

6.2.2 Effect of n/p ratio of the target on the yield of fragments in neutron-rich asymmetric reactions

To investigate the effect of n/p ratio of the target on the yield of various fragments in mass asymmetric reactions with neutron-rich targets, we take same projectile and vary target (by increasing the neutron-richness with increase in the mass). In addition to the above mentioned reactions, we also simulated the reactions of $^{16}_{8}$O + $^{80}_{35}$Br and $^{16}_{8}$O + $^{108}_{47}$Ag. These reactions are taken into account (along with the other reactions as mentioned above) to get a wide range of n/p ratio of targets.

In Figs. 6.5 and 6.6, we display the size of heaviest fragment ($<A_f^{max}>$) and multiplicity of FNs, LCPs and IMFs as a function of n/p ratio of target at two different incident energies (i.e., 50 and 200 Mev/nucleon). From the figures, we observe that the size of the $<A_f^{max}>$ decreases with the corresponding enhancement in the multiplicity of other quantities (FNs, LCPs and IMFs) as one moves from low to high incident energy (i.e., from 50 MeV/nucleon to 200 MeV/nucleon). We also notice that the size of $<A_f^{max}>$

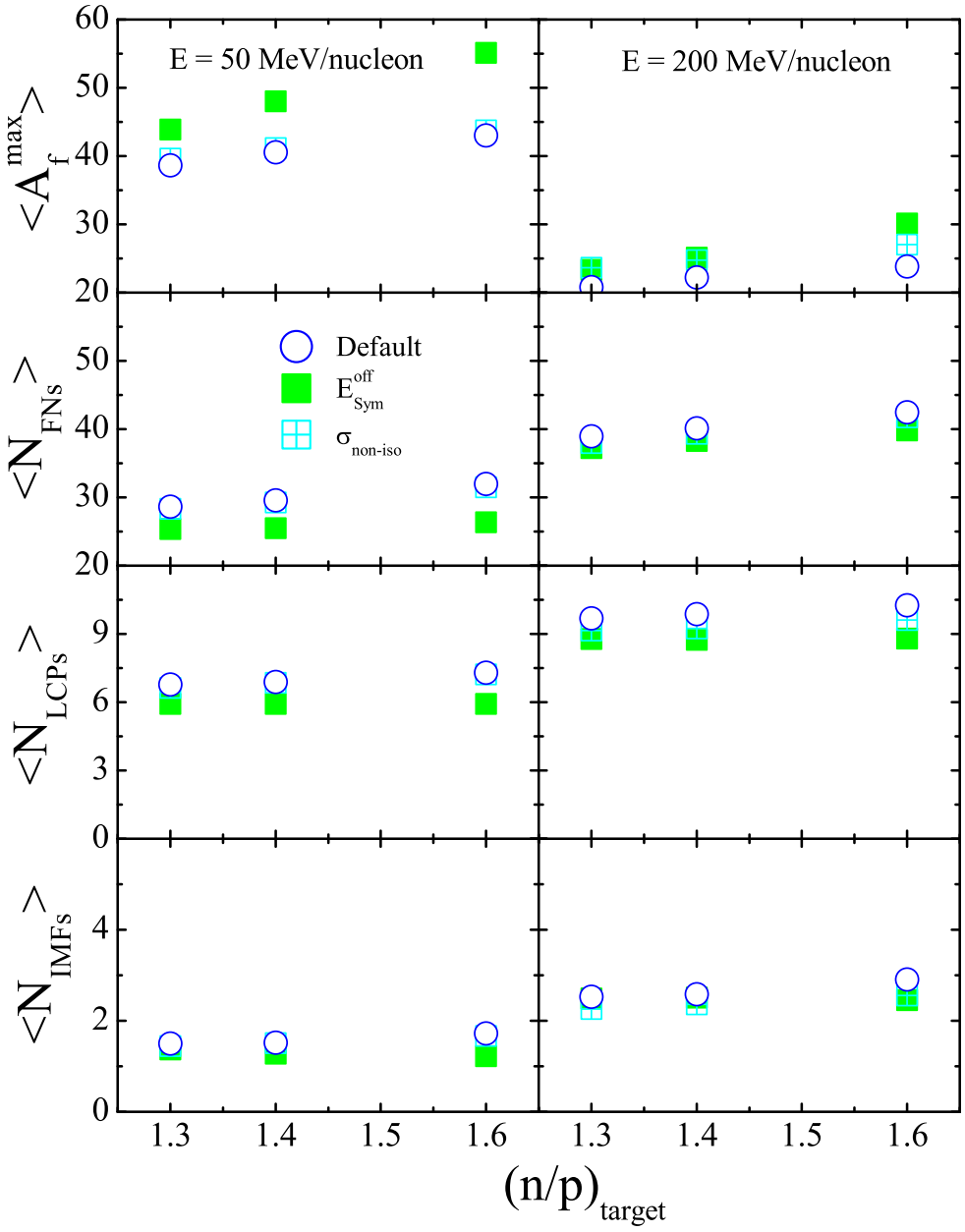

Figure 6.5: The size of heaviest fragment ($<A_f^{max}>$) and the multiplicity of free nucleons (FNs), light charged particles (LCPs) and intermediate mass fragments (IMFs) as a function of n/p ratio of the target for the reactions of $^{16}_{8}$O + $^{80}_{35}$Br/$^{84}_{35}$Br/$^{92}_{35}$Br at two beam energies of 50 (left panels) and 200 (right panels) MeV/nucleon. Various symbols are explained in the text.

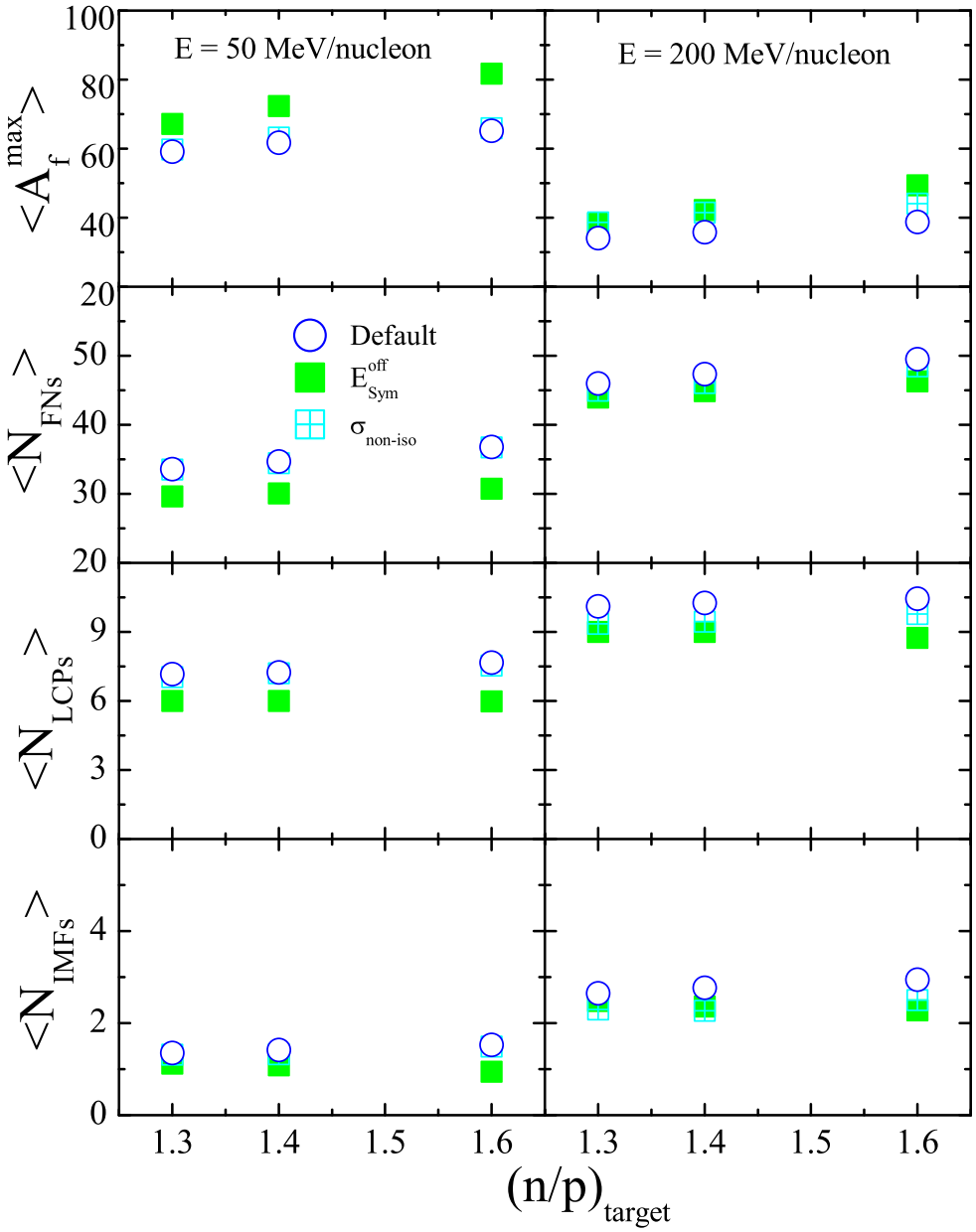

Figure 6.6: Same as Fig. 6.5, but for the reactions of ${}^{16}_{8}\mathrm{O} + {}^{108}_{47}\mathrm{Ag}/{}^{113}_{47}\mathrm{Ag}/{}^{122}_{47}\mathrm{Ag}$.

increases with increase in the neutron content of the target. On the other hand, the yield of different mass fragments (FNs, LCPs and IMFs) shows marginal change with n/p ratio of the target. This happens because with the increase in the n/p of target, the size of the nucleus also increases and thus one gets bigger $<A_f^{max}>$.

Next, we will study the effect of isospin degree of freedom via symmetry energy and NN cross-section on the yield of fragments with increase in the n/p ratio of the target and the results are displayed in Figs. 6.5 and 6.6. From the figures, one finds a bigger $<A_f^{max}>$ with the corresponding decrease in the multiplicity of FNs, LCPs and IMFs when calculations are done without symmetry potential. Moreover, the effect of symmetry energy increases with n/p ratio the of target. We also observe that the role of symmetry energy reduces at higher energy (compare left and right panels of both the figures) as the size of $<A_f^{max}>$ increases by 30% (20%) at 50 (200) MeV/nucleon for the reaction of $^{16}_{8}$O + $^{92}_{35}$Br; when calculations are performed without symmetry potential.

Further, to investigate the role of isospin dependence of the NN cross-section with increase in the n/p ratio of target, we perform the calculations by implementing isospin independent cross section. The results are displayed by crossed squares in Figs. 6.5 and 6.6. From the figures, we find an insignificant role of NN cross-section on the yield of fragments at low beam energy of 50 MeV/nucleon, whereas, marginal effect can be seen at high beam energy of 200 MeV/nucleon for the above mentioned asymmetric reactions.

To see the relative behavior of symmetry potential and isospin-dependent cross-section, in Figs. 6.7 and 6.8, we display the percentage change (from the default calculations) in the size of $<A_f^{max}>$ and yields of FNs, LCPs and IMFs when calculations were performed without symmetry potential and isospin independent NN cross-section. The results are displayed by solid and crossed squares, respectively. The percentage change in the size of $<A_f^{max}>$ is defined as:

$$< \Delta A_f^{max} > (\%) = \Big[\frac{A^{max}_{f(Default)} - A^{max}_{f(E^{off}_{Sym}/\sigma_{noniso})}}{A^{max}_{f(Default)}}\Big] \times 100. \qquad (6.1)$$

Similar, calculations have also been done for the yields of FNs, LCPs and IMFs and the results are displayed in Figs. 6.7 and 6.8. From the figures, we observe that the role of isospin degree of freedom via NN cross-section on the fragmentation is marginal (around 5-10%) whereas, the symmetry energy can alter the dynamics up to 30% when one takes neutron-rich targets in asymmetric colliding nuclei. On the other hand, the effect of symmetry energy increases as n/p ratio of target increases.

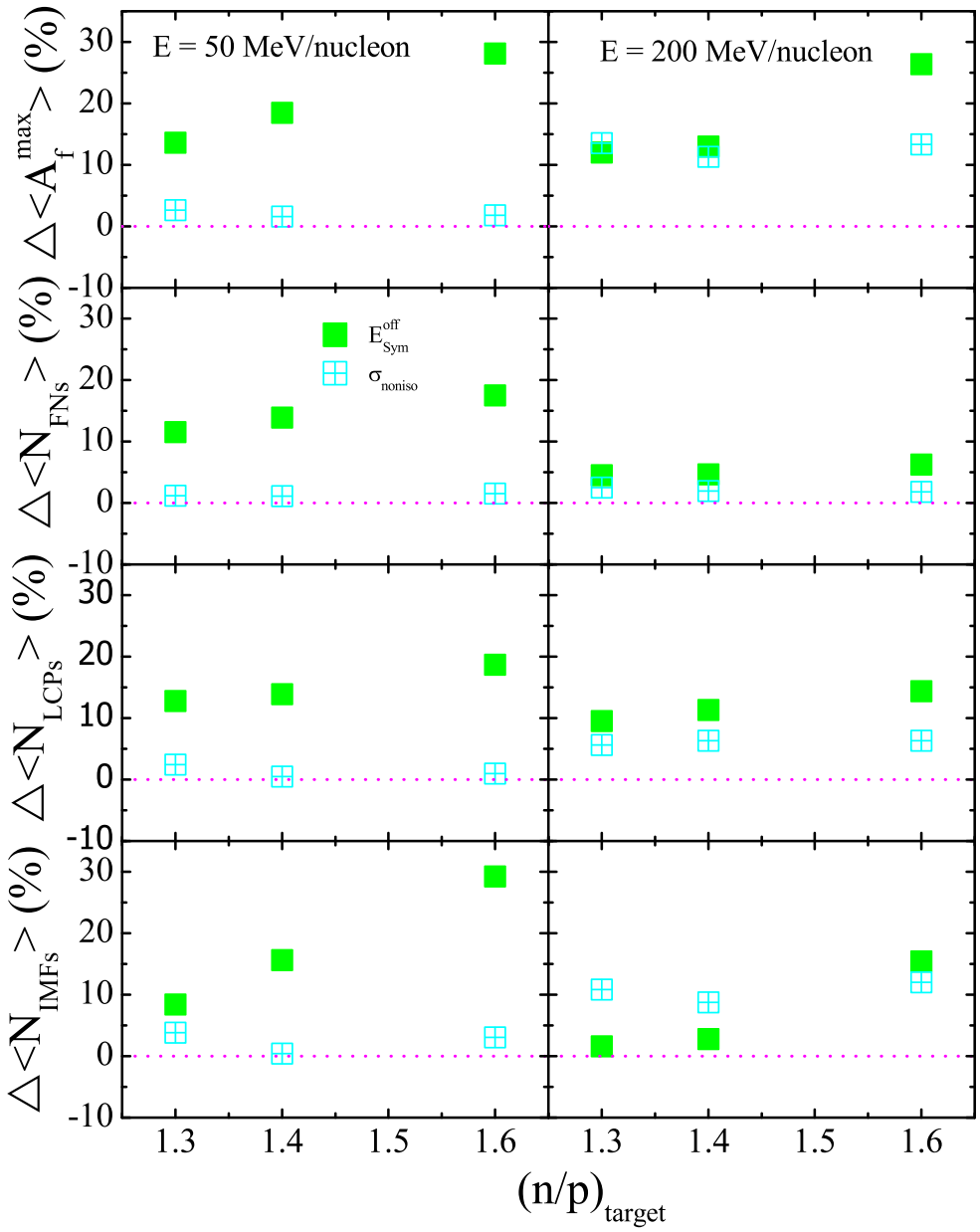

Figure 6.7: The percentage deviations of the size of heaviest fragment ($<A_f^{max}>$) and the multiplicity of free nucleons (FNs), light charged particles (LCPs) and intermediate mass fragments (IMFs) w.r.t. the default calculations for the reactions of $^{16}_{8}$O + $^{80}_{35}$Br/$^{84}_{35}$Br/$^{92}_{35}$Br as a function of n/p ratio of the target. Various symbols are explained in the text.

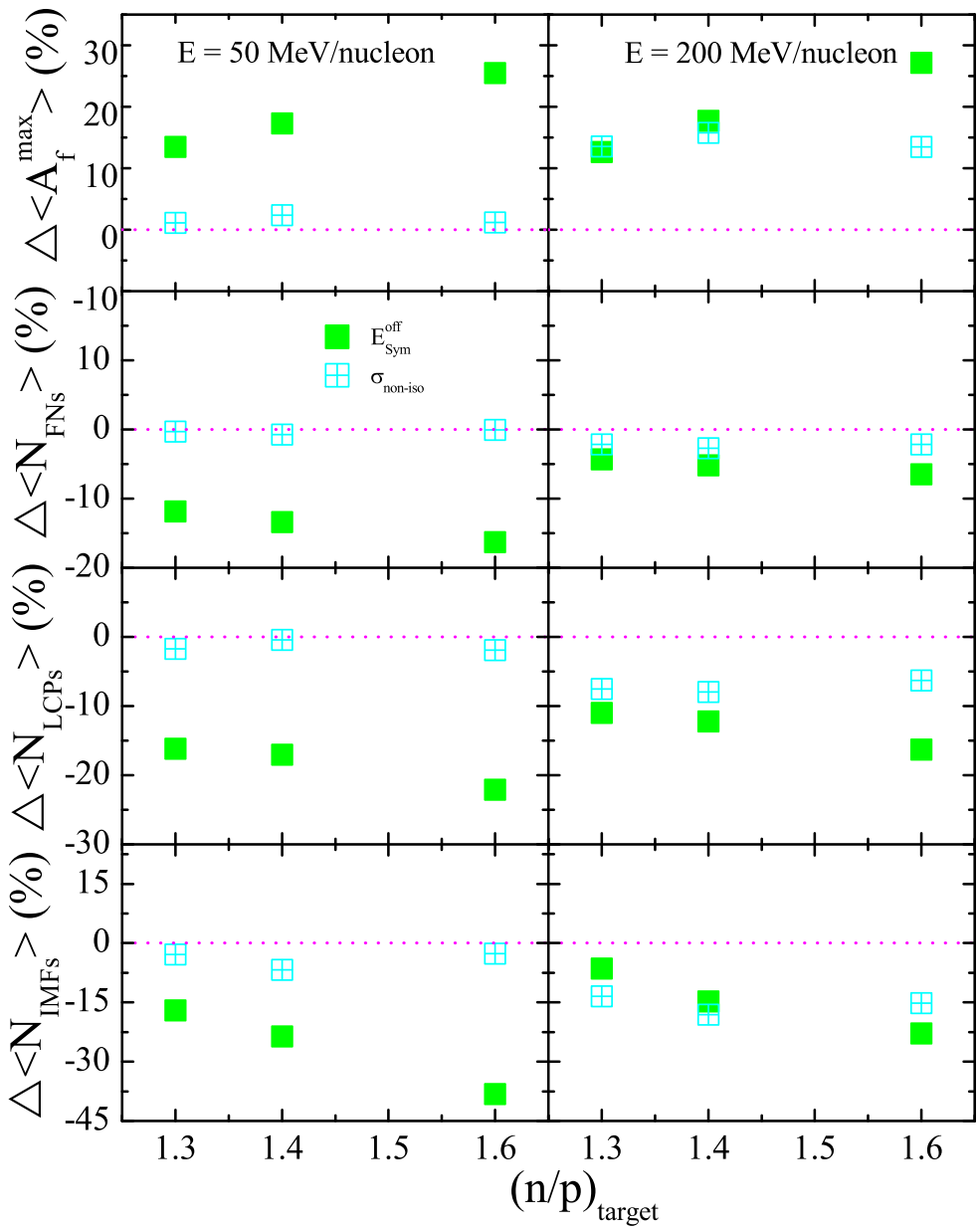

Figure 6.8: Same as Fig. 6.7, but for the reactions of ${}^{16}_{8}\mathrm{O} + {}^{108}_{47}\mathrm{Ag}/{}^{113}_{47}\mathrm{Ag}/{}^{122}_{47}\mathrm{Ag}$.

From the above discussion, it is concluded that symmetry energy affects the dynamics of asymmetric reactions induced by the neutron-rich target. Therefore, study regarding the effect of density dependence of symmetry energy for such collisions would be interesting.

6.2.3 Effect of density dependence of symmetry energy on the asymmetric reactions induced by the neutron-rich nuclei

Here, we will study the role of density dependence of symmetry energy on the dynamics of asymmetric reactions induced by the neutron-rich nuclei and simultaneously we will also compare our calculated results with the ones reported using other approaches. It should be noted that in this regard, studies are very scarce. For example, Fang *et al.* [372] studied the effect of density dependence of symmetry energy on the dynamics of $^{40}_{20}$Ca + $^{124}_{50}$Sn reaction at 140 MeV/nucleon using IBUU model. In particular, the time evolution of maximal baryon density was investigated using two different forms of density dependence of symmetry energy (i.e., $\gamma' = 0.5$ and 0.69). Therefore, we also perform similar calculations for this quantity using our model with same forms. The results are displayed in Fig. 6.9 (left top panel). From the figure (left top panel), one notices that the maximum density reached is more than 1.5 times the normal nuclear matter density. Similar conclusions were also reported by Fang *et al.* [372] where study was performed with IBUU model for the above mentioned reaction. Also, note that in Ref. [372], two chosen forms of density dependence of symmetry energy (with $\gamma' = 0.5$ and 0.69) do not yield much significant variation in results as values of γ' are not very different.

In an another study by Li [363], the role of density dependence of symmetry energy was investigated on the dynamics of $^{100}_{30}$Zn + $^{124}_{50}$Sn and $^{100}_{50}$Sn + $^{124}_{50}$Sn reactions within IBUU model using $\gamma' = 0.5$ and 2. In Fig. 6.9 (left bottom and right panels), we have shown the distribution of free protons as a function of scaled rapidity in the reactions of $^{100}_{30}$Zn + $^{124}_{50}$Sn and $^{100}_{50}$Sn + $^{124}_{50}$Sn at 30 MeV/nucleon for three different colliding geometries of b = 1, 5 and 7 fm using two forms of density dependence of symmetry energy i.e., $\gamma' =$ 0.5 and 2. At sub-saturation region, soft symmetry potential ($\gamma' = 0.5$) is more attractive (for protons) compared to stiffer one ($\gamma' = 2$), therefore, we observe reduced emission of protons with soft symmetry energy compared to stiffer one. Similar behavior was also reported in Ref. [363] using IBUU transport model. Therefore, the above comparisons reveal that for various model ingredients, IQMD model gives consistent results as have

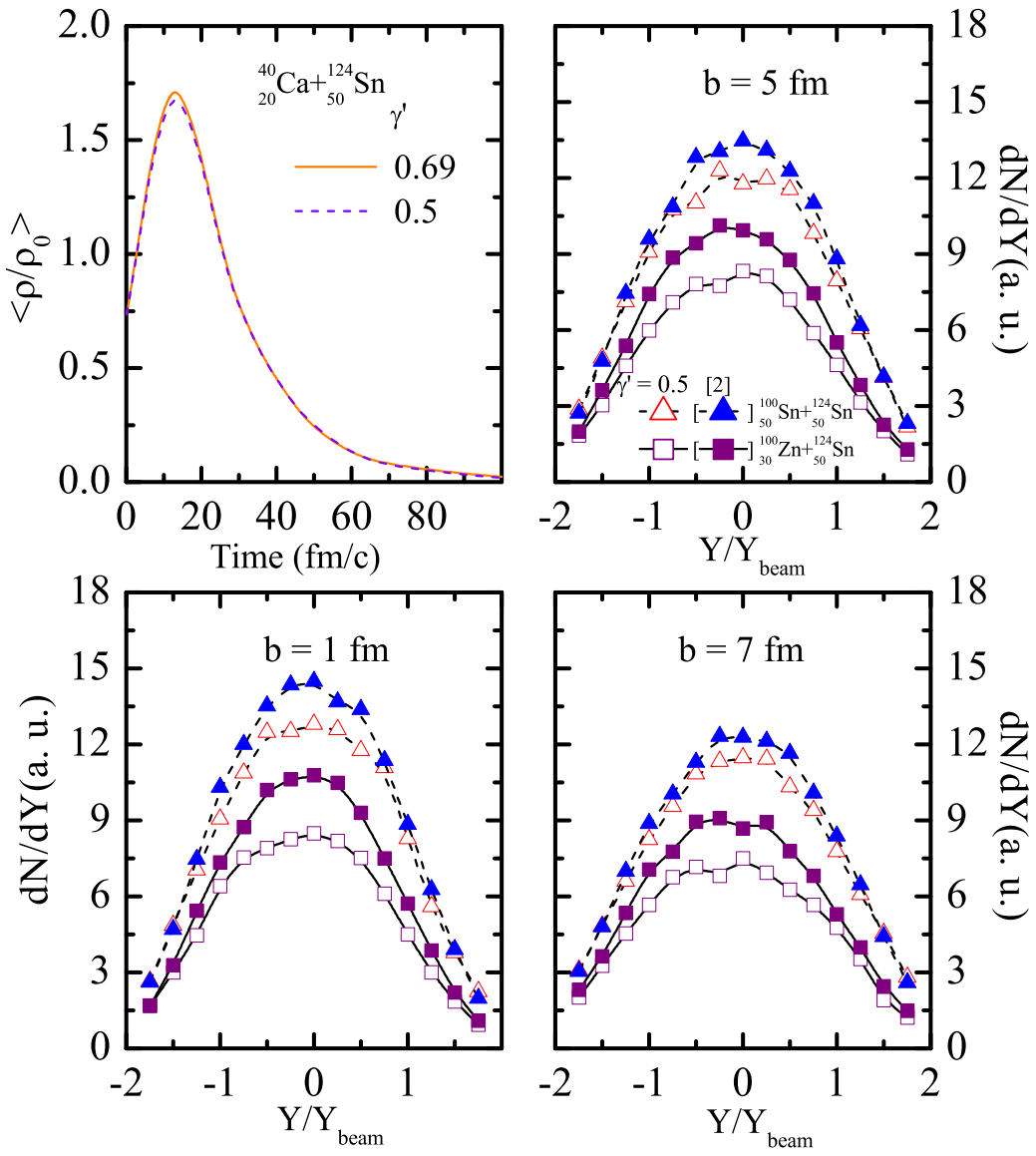

Figure 6.9: (Left top panel) Baryon density as function of reaction time achieved in the central collisions of $^{40}_{20}$Ca+$^{124}_{50}$Sn at 140 MeV/nucleon and (left bottom and right panels) rapidity distribution of protons at 30 MeV/nucleon for different colliding geometries with two forms of density dependence of symmetry energy.

been reported also by other transport models, though, quantitative variation in these findings occur. Also, it is very much clear now that dynamics of asymmetric reactions induced by neutron-rich nuclei is highly sensitive to different model ingredients (such as symmetry energy) and simultaneously isospin degree of freedom plays crucial role for such collisions.

6.3 Summary

We have simulated the heavy-ion reactions for the asymmetric reactions induced by the neutron-rich nuclei to understand the isospin effects with the help of model ingredients (physical parameters) such as symmetry energy and NN cross-section on fragment's yield. We performed a theoretical study within an isospin-dependent quantum molecular dynamics (IQMD) model. We find that symmetry energy alters the dynamics of asymmetric heavy-ion collisions induced by the neutron-rich nuclei at low beam energies and its effect is more pronounced with the increase in the neutron-richness of the target. Whereas, the isospin independent NN cross-section shows marginal effect at higher beam energies for such reactions. This led to conclusion that model ingredients result in considerable change in the dynamics of neutron-rich asymmetric heavy-ion collisions and the fragments's yield is a better probe to study the isospin effects via symmetry energy compared to nucleon-nucleon cross-section for such collisions. Further, our calculations for the baryon density and the rapidity distribution of protons are consistent with other model calculations when one simulates the asymmetric reactions induced by neutron-rich nuclei.